

Deep optical spectroscopy of extended Ly α emission around three radio-quiet $z = 4.5$ quasars ^{*}

F. Courbin¹, P. North¹, A. Eigenbrod¹, and D. Chelouche^{2,**}

¹ Laboratoire d'Astrophysique, Ecole Polytechnique Fédérale de Lausanne (EPFL), Observatoire de Sauverny, CH-1290 Versoix, Switzerland

² Institute for Advanced Study, Einstein Drive, Princeton, NJ 08540, USA

Received xxxxxx/ Accepted xxxxxx

ABSTRACT

We report the first results of a spectroscopic search for Ly α envelopes around three $z \sim 4.5$ radio-quiet quasars. Our observational strategy uses the FORS2 spectrograph attached to the UT1 of the Very Large Telescope (VLT) in the multi-slit mode. This allows us to observe simultaneously the quasars and several PSF stars. The spectra of the latter are used to remove the point-like quasar from the data, and to unveil the faint underlying Ly α envelopes associated with the quasars with unprecedented depth. We clearly detect an envelope around two of the three quasars. These envelopes measure respectively 10'' and 13'' in extent (i.e. 67 kpc and 87 kpc). This is 5 to 10 times larger than predicted by the models of Haiman & Rees (2001) and up to 100 times fainter. Our observations better agree with models involving a clumpy envelope as in Alam & Miralda-Escudé (2002) or Chelouche et al. (2008). We find that the brighter quasars also have the brighter envelopes but that the extend of the envelopes does not depend on the quasar luminosity. Although our results are based on only two objects with a detected Ly α envelope, the quality of the spatial deblending of the spectra lends considerable hope to estimate the luminosity function and surface brightness profiles of high redshift Ly α envelopes down to $F \sim 2 - 3 \times 10^{-21} \text{ erg s}^{-1} \text{ cm}^{-2} \text{ \AA}^{-1}$. We find that the best strategy to carry out such a project is to obtain both narrow-band images and deep slit-spectra.

Key words. Quasars – QSO host galaxy – Ly α envelope – Individual objects: SDSS J0939+0039, BR 1033–0327, Q 2139–4324

1. Introduction

Large-scale Ly α emission ($\sim 10\text{--}100$ kpc) is common among high redshift ($z > 2$) radio galaxies (Villar-Martín 2007). This extended gas shows two components: one is kinematically perturbed by the jets and is part of a jet-induced outflow; the other has a lower velocity dispersion (a few hundreds of km s^{-1} instead of about 1000 km s^{-1}) as well as a fainter surface brightness, but may extend beyond 100 kpc. It has been shown, at least in the case of MRC 2104-242, that the gas is infalling towards the galaxy center (Villar-Martín 2007). This author makes the interesting suggestion that “the radio activity is fed by the infalling gas, so that it is only detected when the infall is happening and efficiently feeding the active nucleus”.

Similar Ly α envelopes (sometimes called “blobs”) are also found around radio-quiet quasars (Steidel et al. 2000; van Breugel et al. 2006; Bunker et al. 2003; Weidiger et al. 2005; Christensen et al. 2006, hereafter CJW). According to the latter authors, Ly α envelopes around radio-quiet quasars (RQQs) are an order of magnitude less luminous than those around RLQs, presumably because the emission of RLQ gaseous envelopes is enhanced by interactions with the radio jets.

Haiman & Rees (2001) have envisaged Ly α emission as a possible constraint on galaxy formation. Gas infalling into the gravitational well of a dark matter halo would be heated, and dissipate this thermal energy partly by collisional excitation of the

Table 1. Journal of observations, along with the main characteristics of the quasars. The apparent magnitudes are given in the AB system. They are computed by integrating the quasar’s spectrum through the RSPECIAL ESO filter curve. The absolute magnitude assumes $H_0 = 72 \text{ km s}^{-1} \text{ Mpc}^{-1}$ and $(\Omega_m, \Omega_\Lambda) = (0.3, 0.7)$.

redshift z	JD(start) −2400000	Exposure time (s)	Airmass	Seeing ('')
SDSS J09395+0039, z=4.490, R(AB)=20.9, M _R =−27.2				
	54203.598	1210	1.18	1.18
	54203.612	1210	1.23	1.24
	54203.631	1210	1.31	1.08
	54203.645	1210	1.40	0.84
	54203.672	1210	1.64	0.86
	54203.686	1210	1.83	0.81
BR 1033-0327, z=4.509, R(AB)=18.5, M _R =−29.6				
	54208.603	1300	1.10	0.88
	54208.618	1300	1.13	1.23
	54236.656	1300	1.17	0.59
	54236.671	1300	1.22	0.47
Q 2139-4324, z=4.460, R(AB)=21.8, M _R =−26.2				
	54326.566	1300	1.41	1.09
	54326.581	1300	1.32	0.98
	54297.632	1300	1.51	1.61
	54297.647	1300	1.40	1.55
	54299.631	1300	1.47	1.29
	54299.647	1300	1.37	1.28
	54319.669	1300	1.10	1.47
	54319.685	1300	1.08	1.48

^{*} Based on observations made with the FORS2 multi-object spectrograph mounted on the Antu VLT telescope at ESO-Paranal Observatory (programme 079.B-0132B; PI: P. North)

^{**} Chandra Fellow

Ly α transition. But the Ly α emission would remain too faint to be detectable at high redshift. However, if a central quasar turns on and photoionizes the gas, the Ly α emission will be much enhanced and should be detectable with present-day instruments. For quasars at redshift $z = 3 - 8$, these authors predict surface brightnesses in the range $10^{-18} < \mu < 10^{-16}$ erg s $^{-1}$ cm $^{-2}$ arcsec $^{-2}$ and angular sizes of a few arcseconds. Alam & Miralda-Escudé (2002) have proposed another theoretical prediction of the Ly α surface brightness of a quasar host galaxy at $z = 3$. They find $\mu = 10^{-17.5}$ and $\mu = 10^{-19.5}$ erg s $^{-1}$ cm $^{-2}$ arcsec $^{-2}$ at angular separations of 0.5'' and 3'' respectively from the quasar. This is much more pessimistic than the estimate by Haiman & Rees (2001), because the authors assume a smaller clumping factor of the cold gas and a Ly α emitting region much smaller than the virial radius. More recently, Chelouche et al. (2007) suggested that quasar nebulae are another manifestation of metal absorption systems associated with L^* galaxies which, by virtue of a nearby quasar, become more efficient Ly α emitter that also scatter Ly α photons from the broad line region of the quasar (BLR). The extent and luminosity of the halo in their model serves as a means to study the nearby environments of quasars and weigh the gaseous content of their halos. To summarize, the study of the emission properties of quasar envelopes provides a promising new means for testing galaxy formation models and various scenarios for the enrichment of the inter-galactic medium.

To explore in more detail the spatial extent, the luminosity and kinematics of the large hydrogen envelopes of remote quasars, we have selected a sample of quasars at redshift $z \sim 4.5$, spanning a broad magnitude range. Before carrying a systematic study of the Ly α envelopes of these quasars, we have obtained deep VLT optical spectra for 3 of them, spanning 3 magnitudes. The present paper describes our observational strategy and our main results, with the detection of a Ly α “nebula” for two of the three quasars.

2. Deep VLT optical spectroscopy

Motivated by the hypothesis that the Ly α emission around quasars is enhanced by the quasar radiation field, our goal is to characterize the properties of the Ly α envelopes as function of the quasar luminosity. The construction of a sample is a compromise between this scientific goal and the technical constraints imposed by the intrinsic faintness of the Ly α envelopes. The observations presented here are intended to demonstrate the feasibility of the project and to give a first characterization of the Ly α envelopes for three quasars with different luminosities.

2.1. Sample and observations

We select bright quasars from the 3rd edition of the SDSS catalogue of quasars (Schneider et al. 2005) and from the 12th edition of the Vérons’ catalogue (Véron-Cetty & Véron 2006). All our targets are at high redshift, i.e., when galaxy formation was still in place. SDSS J0939+0039 and Q 2139–4324 have not been explicitly related to any radio source (Véron-Cetty & Véron 2006) but given their brightness, they are likely RQQs. BR 1033–0327 is an RQQ according to Véron-Cetty & Véron (2006) and Bechtold et al. (2003).

A key observational issue is to avoid both the telluric absorption lines and the numerous atmospheric emission lines in the red part of the optical domain. Residuals of such lines in the sky-subtracted spectra may mimic a Ly α envelope. This latter consideration restricts the accessible redshift range to $4.44 <$

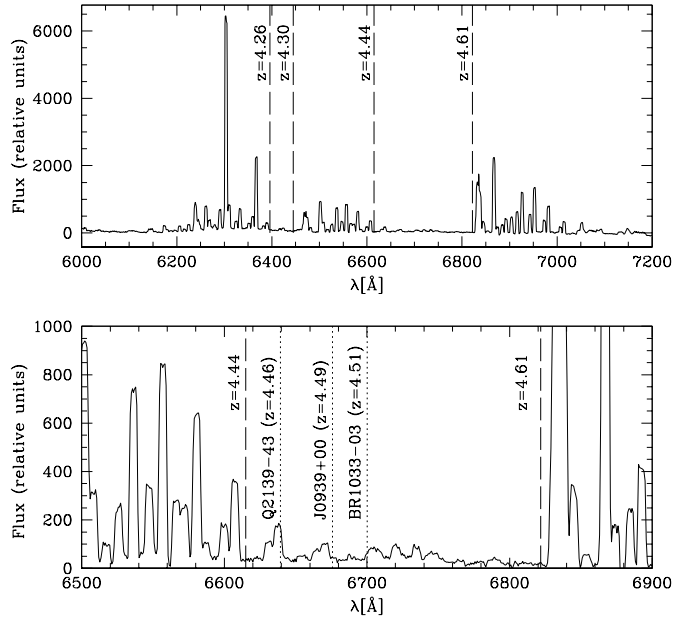


Fig. 1. Spectrum of the sky emission, extracted from our FORS2 data and grism G1200R in combination with a 2''-slit. The full wavelength range accessible to this grism is displayed in the upper panel. A zoom is displayed in the bottom panel, of the region where falls the Ly α emission redshifted at $z \sim 4.5$. The positions of the Ly α line of the three quasars are also indicated.

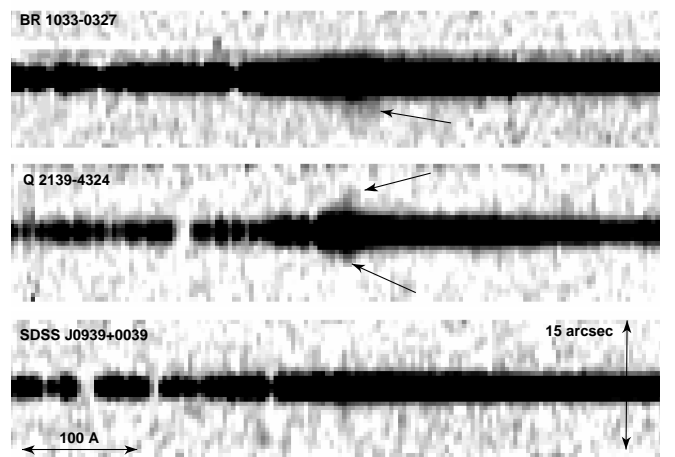


Fig. 2. The combined and sky-subtracted FORS2 spectra for the three quasars, prior to any deconvolution (see text). The images have been binned by 5 pixels in the spectral direction (i.e., the new pixel size is 3.8 Å) and by 2 pixels in the spatial direction, resulting in a pixel size of 0.5''. The extended Ly α emission is indicated with arrows in two of the objects.

$z < 4.61$, as shown in Fig. 1, with an additional small window at $4.26 < z < 4.30$. Finally, there must be adequate nearby stars with about the same brightness as the quasar in order to carry out a careful subtraction of the quasar’s light using image deconvolution, as described in Courbin et al. (2000).

The observations were carried out in ESO Period 79 (April–September 2007) in service mode with the FORS2 multi-object spectrograph attached to VLT-UT1. The ESO grism G1200R+93

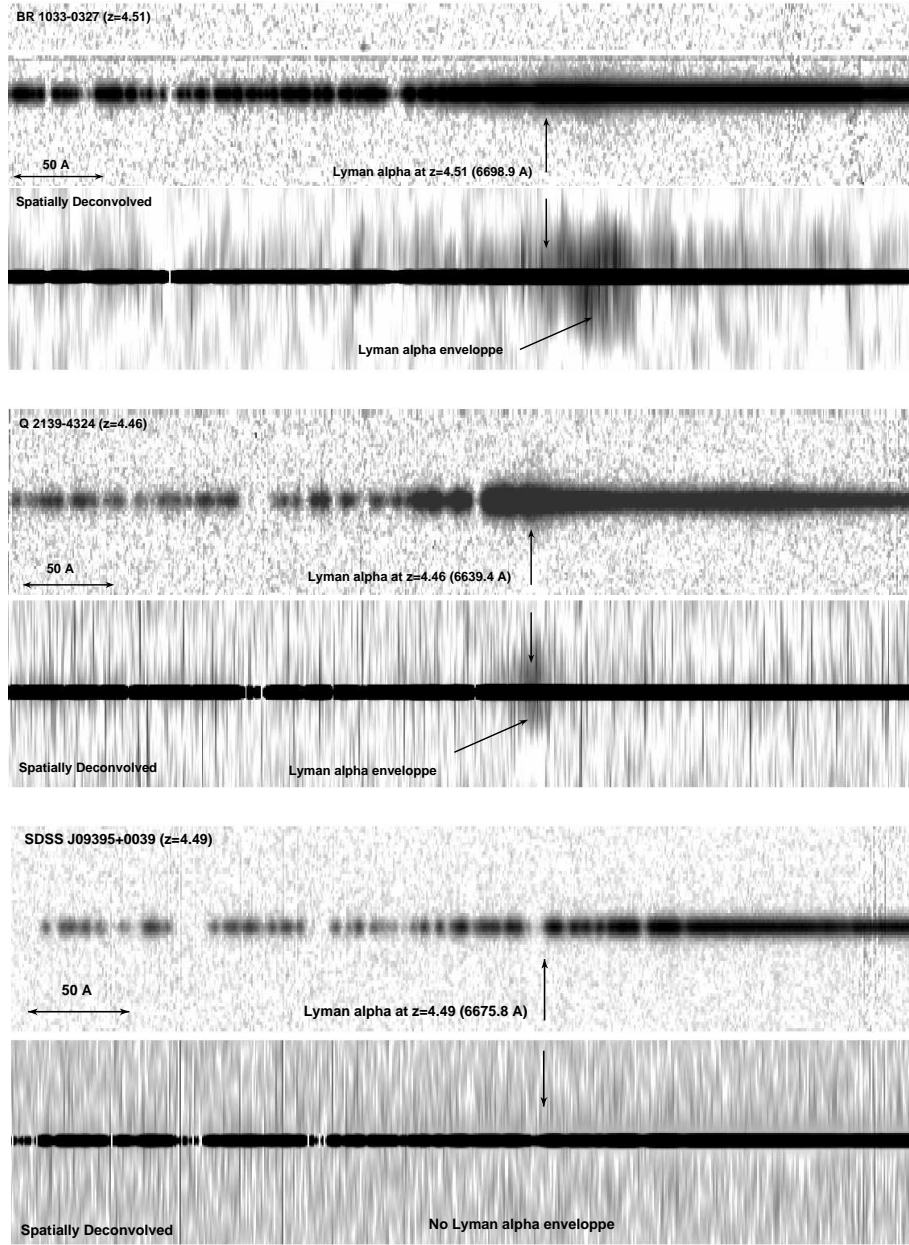


Fig. 3. The three combined and sky-subtracted FORS2 spectra along with their spatial deconvolution. The spatial resolution after deconvolution is $0.25''$. In each panel, the vertical arrow indicates the position of the Ly α emission line of the quasar. A Ly α envelope is detected in two quasars out of three. The envelope of BR 1033–0327 is redshifted compared with the quasar. The height of the spectra is $16''$ in all panels.

has a resolving power $R = 1070$ with a $2''$ -slit, ensuring to catch most of the flux of the Ly α envelope. This grism is used in combination with the GG435+81 order separating filter, leading to the wavelength coverage $6000 \text{ Å} < \lambda < 7200 \text{ Å}$. The maximum efficiency of this combination coincides well with the expected wavelength of the redshifted Ly α line, i.e. about 6686 Å .

The multi-slit MXU mode is used, with slits that are long enough (typical length: $\sim 20''$) to reliably model and subtract the sky emission. Although only one scientific target is observable in each field, we use the MXU capability in order to observe several stars through identical slits. In this way, a spectrum PSF is measured simultaneously with the quasar. This is crucial for the spatial deconvolution of the data to work efficiently (Courbin et al. 2000) and to separate well the quasar spectrum from that of the putative envelope.

Although the requested maximum seeing is $0.9''$ for our observing programme, this condition is fulfilled in practice for three Observing Blocks (OBs) out of the nine executed. Each planned OB consists of one short acquisition image, followed by two long exposures for spectroscopy. The planned total exposure time for each object is 2.7 hours, with seeing better than $0.9''$. The journal of the actual observations is presented in Table 1.

2.2. Reduction and spatial deconvolution

The data reduction is straightforward. It is carried out using the standard IRAF procedures. The individual spectra listed in Table 1 are flatfielded using dome flats, and then wavelength-calibrated in two dimensions in order to correct the sky emission lines for slit curvature. The scale of the reduced data is 0.76 Å

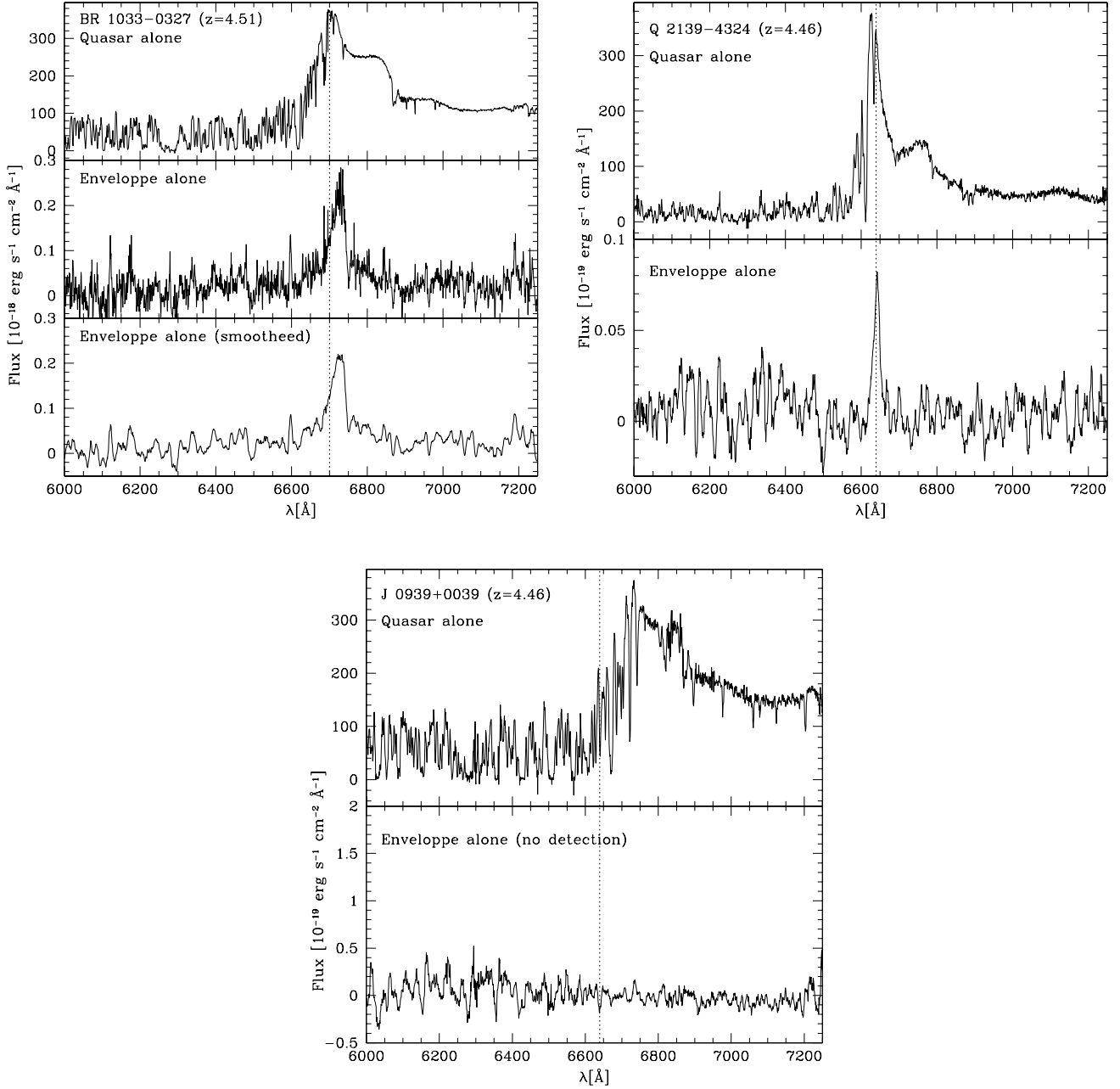


Fig. 4. Extracted 1D spectra for the three quasars. In each case, the top panel shows the quasar alone and the bottom panel shows the Ly α envelope alone, after spatial deconvolution of the spectra. The vertical dotted line indicates the position of the un-absorbed Ly α emission line, at the redshift of the quasar. In all cases, the spectrum of the Ly α envelope has been smoothed using a boxcar of 8 Å. In the case of BR 1033–0327 we also display the un-smoothed spectrum (middle panel), as the signal-to-noise is higher than in the other two objects.

Table 2. Main properties of the Ly α envelopes, as measured on the spectra of Fig. 4. All parameters are given in the observer’s frame. The $1 - \sigma$ detection limit is the standard deviation of the background noise (after smoothing with a car box of 8 Å) integrated along the whole slit. Note that the surface brightness is integrated in wavelength but given per arcsec², while the $1 - \sigma$ limit is spatially integrated but given per Å.

Object	λ [Å]	mean F_λ [erg s ⁻¹ cm ⁻² Å ⁻¹]	FWHM [Å]	Extent ('', kpc)	Surface brightness [erg s ⁻¹ cm ⁻² '' ⁻²]	$1 - \sigma$ detection limit [erg s ⁻¹ cm ⁻² Å ⁻¹]
BR 1033–0327	6725.0 ± 0.5	$4.0(\pm 0.4) \times 10^{-19}$	50 ± 10	13, 86	$7.7(\pm 0.8) \times 10^{-19}$	2.7×10^{-20}
Q 2139–4324	6641.0 ± 0.3	$7.2(\pm 1.4) \times 10^{-21}$	22 ± 2	10, 66	$8.0(\pm 1.6) \times 10^{-21}$	2.5×10^{-21}
SDSS J0939+0039	—	—	—	—	—	2.0×10^{-20}

Table 3. Ly α luminosity of the quasar in the BLR, compared with the luminosity of the extended envelope. The flux in the quasar BLR is measured in the wavelength interval 1200–1230 Å (rest-frame). The last two lines give the Ly α flux of the envelope, after correction by slit-clipping (see text).

Object	L(BLR) [erg s ⁻¹]	L(Ly α) [erg s ⁻¹]
BR 1033–0327	$7.2(\pm 0.4) \times 10^{45}$	$4.0(\pm 0.4) \times 10^{42}$
Q 2139–4324	$4.6(\pm 0.2) \times 10^{44}$	$3.0(\pm 0.6) \times 10^{40}$
SDSS J0939+0039	$4.1(\pm 0.2) \times 10^{44}$	–
BR 1033–0327	–	$2.0(\pm 0.2) \times 10^{43}$
Q 2139–4324	–	$1.2(\pm 0.3) \times 10^{41}$

per pixel in the spectral direction and 0.25'' in the spatial direction.

The sky emission is then subtracted from the individual frames by fitting a second order polynomial along the spatial direction. This fit considers only the 10 pixels on each side of the slit and the sky at the position of the quasars is interpolated using this fit, both on the quasar and on the PSF stars.

The cosmic rays are removed using the L.A. Cosmic algorithm (van Dokkum 2001). All the frames are checked visually after this process in order to make sure that no signal is mistakenly removed from the data. Particular care is paid to the good seeing frames, where the central parts of the quasar and of the PSF stars must not be misidentified with cosmic rays.

Even though FORS2 has an atmospheric refraction corrector, the shape of the spectra along the spectral direction shows slight distortions, i.e., the position of the spectrum changes as a function of wavelength. These distortions are corrected for and the spectra are eventually weighted so that their flux is the same at a reference wavelength, before they are combined into a deep 2D spectrum. We show in Fig. 2 the combined spectra of the three quasars, after binning both in the spatial and the spectral directions. An extended Ly α envelope is already visible up to 4'' away from the quasars in two objects: BR 1033–0327 and Q 2139–4324.

While a Ly α envelope is visible on the combined data already, measuring its actual flux requires accurate spatial deblending. We carry out this delicate task by spatially deconvolving the spectra following the method described in Courbin et al. (2000). This method is an adaptation to spectroscopy of the “MCS” image deconvolution algorithm (Magain et al. 1998). It has been used successfully on many occasions. Among others, the algorithm has been used in order to unveil the spectrum of the lensing galaxy in multiply imaged quasars (Eigenbrod et al. 2007) and to study low redshift quasar host galaxies (Letawe et al. 2007).

The results of the present application to high redshift quasars are displayed in Fig. 3. The algorithm uses the spatial information contained in the spectrum of several PSF stars in order to sharpen the data in the spatial direction. At the same time, it also decomposes the data into a point-source and an extended-source channel. The output of the deconvolution procedure consists of two individual spectra, one for the quasar and one for its host galaxy (or Ly α envelope), free of any mutual light contamination. It is therefore possible to estimate the luminosity of the Ly α emission “underneath” the quasar. Subsampling of the data is also possible with the MCS algorithm, hence the pixel size in Fig. 3 is half that of the original data, i.e., the new pixel size is 0.125''.

3. Results

The main scientific information in our data is the Ly α luminosity of the envelopes, their angular size, and their mean surface brightness. The measurements of the spectra shown in Fig. 4 are presented in Tables 2 & 3. To check the flux calibration of the deconvolved spectra, we integrate them in the FORS2 RSPECIAL filter. This filter is also used to obtain short acquisition images prior to the long spectroscopic exposures. These “spectroscopic” AB magnitudes are given in Table 1. We check that they are compatible with the simple aperture photometry obtained from the short images.

We detect a Ly α envelope in 2 out of 3 objects. Our flux limit (integrated over the whole object) is very faint, as indicated in Table 2, up to two orders of magnitude fainter than previous studies in this field (Christensen et al. 2006; Bremer et al. 1992). Note, however, that our limit is computed by integrating the spectrum over the full extent of the Ly α envelope.

The measurable extent of the envelopes is $r \sim 43$ kpc for BR 1033–0327 and $r \sim 33$ kpc for Q 2139–4324, measured from the quasar’s centroid to the faintest visible isophote, i.e., at the detection limit as given in Table 2.

While the surface brightness of the Ly α fuzz is not affected by slit losses, the total luminosity is. Assuming that the Ly α envelopes are uniform face-on disks with diameters equal to the extents quoted in Table 2, we can estimate the amount of flux missed by using a slit width of 2''. The observed luminosities of the Ly α envelopes for BR 1033–0327 and Q 2139–4324 are given in Table 3 as well as the luminosities after the correction for the slit clipping.

The velocity of the Ly α envelope in Q 2139–4324 is well compatible with that of the quasar. However, the extended Ly α emission in BR 1033–0327 is redshifted by $\Delta\lambda = 26 \pm 5$ Å, i.e., $\Delta V = +1165 \pm 225$ km s⁻¹ with respect to that of the quasar. We have checked our deconvolution using several PSF stars and using different smoothing terms (see Courbin et al. 2000). These checks leave the observed shift unchanged. An explanation for this line shift may be that the redshift of the quasar is incorrect, as it is measured only from the Ly α line itself and from the C IV and C III] lines. The Ly α emission of the quasar is strongly affected by the Ly α forest, and the carbon lines in quasars are known to be blueshifted with respect to the actual redshift of the quasar. Using infrared observations, where the quasar [O III] narrow line is accessible at moderate redshifts, McIntosh et al. (1999) find an average blueshift of 860 km s⁻¹ and 600 km s⁻¹ of the C IV and C III] broad lines with respect to the [O III] line. A similar conclusion is drawn by Richards et al. (2002) using SDSS quasar spectra. The velocity shift we observe between the quasar and the Ly α envelope of BR 1033–0327, although large, is still compatible with a biased redshift measurement of the quasar.

3.1. Redshift dependence

The observed surface brightness of the two Ly α envelopes detected here is fainter by about 1–2 orders of magnitude compared to the CJW objects. This difference cannot be explained solely by the different redshift ranges of the two samples. While our sample is at $z_1 \sim 4.5$, most of the objects in CJW are at $z_2 \sim 3.3$ and so the flux ratio by redshift dimming alone would be $F(z_2)/F(z_1) = (1+z_2)^4/(1+z_1)^4 \sim 2.7$, i.e., much smaller than the observed ratio.

Taken at face value, our sample as a whole finds that higher- z objects tend to have smaller surface brightnesses. Nevertheless,

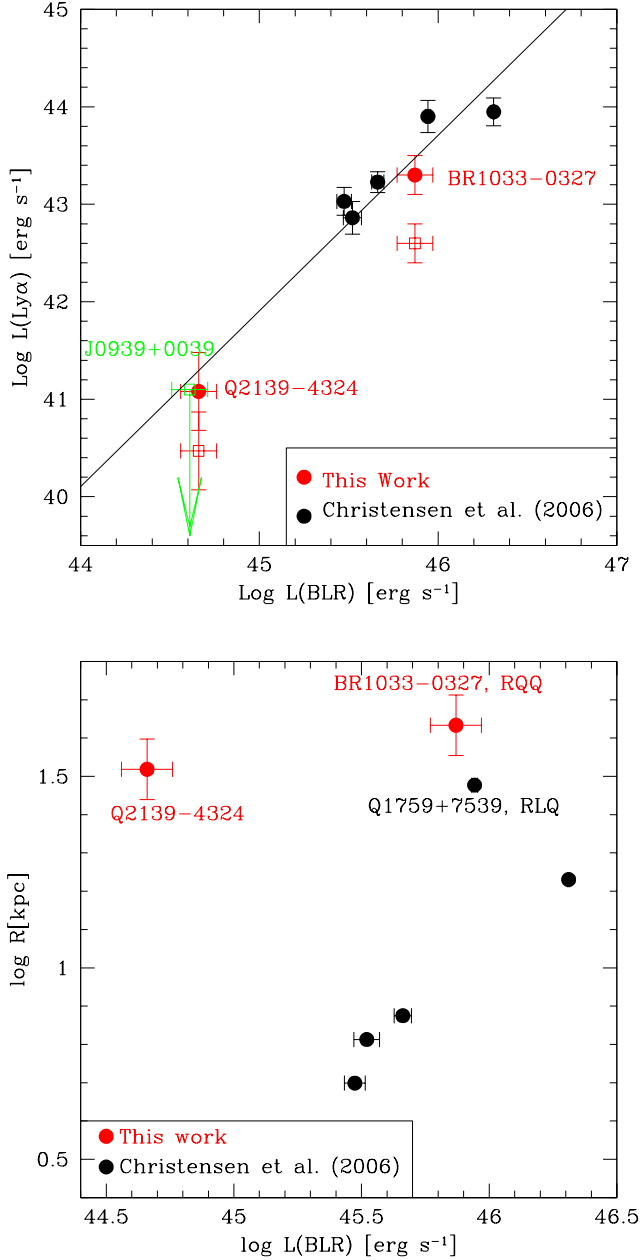


Fig. 5. *Top:* relation between the total luminosity of the Ly α envelopes and that of the quasar in the broad Ly α line. Our measurements are compared with CJW. The open symbols represent the direct measurements while the filled symbols are corrected for slit clipping (see text). The green symbols show our upper limit for SDSS J0939+0039, where no Ly α envelope is seen. In doing this, we assume a size $r=33$ kpc (i.e., the mean size of the two other objects) and we do not correct for slit-clipping. *Bottom:* the radius of the envelope as a function of $L(\text{BLR})$. Note the tight trend followed by the envelopes of the bright RQQs of CJW, and the different behavior of the envelopes of the fainter quasar Q 2139–4324. Note also that BR 1033–0327 stands above the maximum size of the objects of CJW, likely due to our deeper flux limit.

it is important to note the possibly strong dependence of the envelope properties on the object luminosity (see below). In particular, only one object (BR 1033–0327) in our sample overlaps

with the luminosity range probed by CJW, and its surface brightness cannot be rejected at the $3 - \sigma$ level from being drawn from the same sample (where σ is the standard deviation and the t -test performed on the logarithm of the quantities rejects the object at the 94% level). The two other objects in our sample do have significantly lower surface brightness, at the 99.8% confidence according to t -test. This is a lower limit given the upper limit on the undetected envelope in SDSS J0939+0039. However, the quasar luminosities are also lower by almost an order of magnitude relative to the faintest object in CJW.

One potential concern is whether our observations artificially find larger envelopes than CJW just because they are deeper. We note, however, that the mean size of the envelopes in our sample is ~ 38 kpc compared to 26.4 kpc in CJW’s sample, which could account for a 50% difference in area but not for an order of magnitude effect.

3.2. Dependence upon the luminosity of the quasar

While the surface brightness of the Ly α envelopes in our small sample of 3 objects is much lower than the observations of CJW, their total luminosities agree much better.

We show in Fig. 5 the luminosity-luminosity diagram, comparing the total flux in the Ly α envelope as a function of the quasar’s luminosity in the broad Ly α line. After correcting for slit-clipping, we find that our points, combined with the ones of CJW, follow the linear relation:

$$\text{Log}[L(\text{Ly}\alpha)] = 1.8 \times \text{Log}[L(\text{BLR})] - 39.2 \quad (1)$$

This fit considers a mix of objects at redshifts $z \sim 3$ and $z \sim 4.5$, i.e., we assume no strong redshift evolution of the luminosity of the envelopes. We do not include in the fit our upper limit for SDSS J0939+0039 although the data point is shown in Fig. 5. The depth of our observations for this object is consistent with the trend found by using the 5 points of CJW and our 2 objects with a positive detection of a Ly α envelope. Our new observations for the 3 objects therefore seem to support the fact that brighter quasars also have brighter Ly α envelopes, under the assumption of negligible redshift evolution.

The relation between the size of the envelope and the quasar luminosity is much less clear. CJW find a trend that brighter RQQs also display larger envelopes. In our sample we find no such trend, as shown in Fig. 5. The main difference between the observations of CJW and ours is depth. With our deeper observations, we probe Ly α envelopes much further away from the quasar than CJW. In addition the small field of view used in CJW implies severe clipping of the envelopes, if they extend much beyond a few arcsecs. This may also be at the origin of the discrepant surface brightnesses between CJW and the present work.

4. Comparison with models and future prospects

Current models for the emission of quasar envelopes are in their infancy and estimates for the observable properties of such objects depend on several tunable parameters such as halo mass, clumping factor for the gas, quasar luminosity, metallicity, as well as redshift (Haiman & Rees 2001; Alam & Miralda-Escudé 2002; Chelouche et al. 2007). This limitation, as well as the size of current samples and the parameter range covered, make a quantitative comparison with current models unwarranted. In addition, our results may be partly contaminated by emission from excited inter stellar medium in the host galaxy of the quasar; an

effect not accounted for by current models. Nevertheless, several qualitative observations may be made.

The flux level observed from the envelopes of bright quasars seem to indicate that such objects inhabit halos which are more massive in terms of their gaseous content (and possibly total mass) than those of L^* galaxies (Alam & Miralda-Escudé 2002; Chelouche et al. 2007). Further support for this conclusion comes from study of bright quasars at low redshifts Serber et al. (2006). The new results presented here for the less luminous quasars indicate that the surface brightness is lower than the predictions of Haiman & Rees (2001) for all relevant halo masses (see their Fig. 2). Within the framework of their model this suggests a rapid evolution of those systems already at $z > 4.5$, i.e. the cold gas has been converted to stars (or into a thin disk) already at $z \sim 4.5$. As a consequence, there is not enough gas left when the quasar turns on, to reprocess the quasar light into detectable Ly α emission.

Our results seem to indicate a much more complex picture than is portrayed by current models. To be able to make some progress and to quantitatively compare data and models it is necessary to gain better information concerning:

- The surface brightness profile of quasar envelopes. This will allow to make a better distinction between recombination flux and photon scattering models as well as to understand the origin of the gas and possible link with absorption-line systems associated with galaxies (Alam & Miralda-Escudé 2002; Chelouche et al. 2007).
- The gas metallicity (via the detection of e.g., N V λ 1240 line). This would provide an essential clue to the origin of the gas and whether or not it is considerably enriched. It may also reveal whether the cooling time-scales and gas densities assumed in different models are realistic.
- Dependence of envelope observables on quasar properties. This will allow us to discriminate between the effect of environment and that of quasar luminosity on the properties of the envelope thereby allowing us to constrain its physics.

So far, the observational material available to study Ly α envelopes of RQs is extremely scarce, with a mere half-dozen objects with different redshifts and observed with different instruments, down to very different depths.

Our deep slit-spectroscopy observations show that a homogeneous sample of quasars with redshift up to $z=4.5$ can be built in a reasonable amount of telescope time. In addition, our finding that Ly α envelopes can be surprisingly large ($r \sim 10$ - $15''$) and faint, make integral field spectroscopy a poor solution to undertake this task, due to poor cosmetics and sensitivity. A more viable option is to conduct a two-step programme focusing on 1- narrow-band imaging of RQs at different redshift slices in order to map surface brightness profiles for the Ly α envelopes of quasars with a broad range luminosities and 2- to carry out deep slit-spectroscopy with well controlled slit-clipping, with high spectral resolution and with very deep flux limit. The latter shall provide us with the additional metallicity and velocity information required to constrain models.

Acknowledgements. We would like to thank Dr. Lise Christensen for providing us with the electronic form of the Tables in CJW and Anne Verhamme for useful discussions. This study is supported by the Swiss National Science Foundation.

References

Alam, S. M. K. & Miralda-Escudé, J. 2002, ApJ, 568, 576
Bechtold, J., Siemiginowska, A., Shields, J., et al. 2003, ApJ, 588, 119

Bremer, M. N., Fabian, A. C., Sargent, W. L. W., et al. 1992, MNRAS, 258, 23
Bunker, A., Smith, J., Spinrad, H., Stern, D., & Warren, S. 2003, Ap&SS, 284, 357
Chelouche, D., Ménard, B., Bowen, D. V., & Gnat, O. 2007, ArXiv e-prints, 706
Christensen, L., Jahnke, K., Wisotzki, L., & Sánchez, S. F. 2006, A&A, 459, 717
Courbin, F., Magain, P., Kirkove, M., & Sohy, S. 2000, ApJ, 529, 1136
Eigenbrod, A., Courbin, F., & Meylan, G. 2007, A&A, 465, 51
Haiman, Z. & Rees, M. J. 2001, ApJ, 556, 87
Letawe, G., Magain, P., Courbin, F., et al. 2007, MNRAS, 378, 83
Magain, P., Courbin, F., & Sohy, S. 1998, ApJ, 494, 472
McIntosh, D. H., Rix, H.-W., Rieke, M. J., & Foltz, C. B. 1999, ApJ, 517, L73
Richards, G. T., Vanden Berk, D. E., Reichard, T. A., et al. 2002, AJ, 124, 1
Schneider, D. P., Hall, P. B., Richards, G. T., et al. 2005, AJ, 130, 367
Serber, W., Bahcall, N., Ménard, B., & Richards, G. 2006, ApJ, 643, 68
Steidel, C. C., Adelberger, K. L., Shapley, A. E., et al. 2000, ApJ, 532, 170
van Breugel, W., de Vries, W., Croft, S., et al. 2006, AN, 327, 175
van Dokkum, P. G. 2001, PASP, 113, 1420
Véron-Cetty, M.-P. & Véron, P. 2006, A&A, 455, 773
Villar-Martín, M. 2007, New Astronomy Reviews, 51, 194
Weidiger, M., Moller, P., Fynbo, J. P. U., & Thomsen, B. 2005, A&A, 51, 194